Clays and Clay Minerals, Vol. 57, No. 3, 279–289, 2009.

SELECTIVITY OF Co AND Ni BY K-DEPLETED MICAS

YUNCHUL CHO[1], SRIDHAR KOMARNENI[2,*], AND SANG-IL CHOI[3]

[1] Peter A. Rock Thermochemistry Laboratory and NEAT ORU, University of California at Davis, Davis, CA 95616, USA
[2] Department of Crop and Soil Science and Materials Research Institute, The Pennsylvania State University, University Park, PA 16802, USA
[3] Department of Environmental Engineering, Kwangwoon University, 447-1, Wolgye-Dong, Nowon-Gu, Seoul, South Korea

Abstract—Contamination of the environment with heavy metals, including cationic radionuclides, is a serious problem which has yet to be fully overcome. A class of potentially effective cation exchangers for sequestering heavy metals which has received little attention is K-depleted mica. The purpose of this study was to investigate the heavy-metal cation exchange properties of K-depleted phlogopite and biotite, which were prepared from a natural phlogopite and biotite, respectively, using sodium tetraphenylborate (NaTPB). The X-ray diffraction (XRD) patterns showed that interlayer K^+ ions were completely replaced with exchangeable Na^+ ions, resulting in the expansion of the d_{001} spacing of both K-depleted phlogopite and K-depleted biotite. In order to investigate the cation exchange selectivity of K-depleted phlogopite and biotite for Co^{2+} and Ni^{2+}, cation exchange isotherms and Kielland plots were constructed. The isotherms and Kielland plots indicated that both K-depleted phlogopite and biotite are highly selective for Co^{2+} as well as Ni^{2+}. The XRD patterns after both $2Na^+ \rightarrow Co^{2+}$ and Ni^{2+} exchange reactions suggest that double sheets of interlayer water are present in the interlayer. These K-depleted micas are potential cation exchange materials for removal of some heavy metals such as Ni and radioactive species such as ^{60}Co from solution.

Key Words—Heavy-metal Cation, Ion Exchange, K-depleted Biotite, K-depleted Phlogopite.

INTRODUCTION

Contamination of groundwater and soils by heavy metals is a serious environmental concern. Some heavy metals such as Cr, Co, Ni, Cu, and Zn are considered as toxicologically interesting elements (Crosby, 1998). Among those heavy metals, Co has received considerable attention because of its geochemical behavior (Charlet and Manceau, 1994). Cobalt is readily adsorbed on Fe and Mn oxides and on phyllosilicate minerals (Means *et al.*, 1978a; Schlegel *et al.*, 1999). Cobalt adsorption on the minerals limits its mobility in soils. Adsorption of Co in the presence of organic ligands decreases, however, due to the formation of complexes, resulting in the increase of Co solubility and mobility (Means *et al.*, 1978b). The transport and fate of ^{60}Co radioactive isotopes in the environment is important because it is often found in radionuclide-contaminated sites (Killey *et al.*, 1984; Olsen *et al.*, 1986; Blom *et al.*, 1991). Nickel has also received considerable attention because of the presence of many Ni-bearing silicates, such as serpentine, in soils (Crosby, 1998; Brady and Weil, 2002). Both Ni and Co have been used widely as industrial catalysts; Ni in mining, electroplating, pigments, and the battery industry (Asku, 2002); and Co in electroplating, pigments, and the metal alloy industry (Rengaraj and Moon, 2002).

* E-mail address of corresponding author:
komarneni@psu.edu
DOI: 10.1346/CCMN.2009.0570301

Numerous studies of the removal of heavy metals from water and soil have been carried out. Several treatment technologies such as precipitation, ion exchange, adsorption, and reverse osmosis have been proposed and investigated (Blanchard *et al.*, 1984; Netzer and Hughes, 1984; Strelko and Malik, 2002). Of these, ion exchange has received considerable attention (Blanchard *et al.*, 1984; Ganesan and Walcarius, 2004; Coleman *et al.*, 2006). Development of cost-effective ion exchangers has received a great deal of interest: organo-silica (Ganesan and Walcarius, 2004), mica (Bortun *et al.*, 1998), kaolinite (Suraj *et al.*, 1998), Na-4 mica (Kodama and Komarneni, 1999), zeolite (Chang and Shih, 2000), and titanosilicate (Lv *et al.*, 2004). Of those ion exchangers, chemically modified mica such as K-depleted mica (Na-mica) is found to be an excellent inorganic ion exchanger for radioactive species (Cs and Sr) as well as alkali and alkaline earth metal ions. Komarneni and Roy (1988) first reported that K-depleted phlogopite (Na-phlogopite) is highly selective for Cs and able to immobilize Cs in the interlayers. Stout *et al.* (2006) showed that the K-depleted phlogopite is selective for Cs as well as Sr. Bortun *et al.* (1998), on the other hand, showed that Na-phlogopite and Na-biotite are selective for alkali and alkaline earth metal ions. Many studies of alkali and alkaline earth metal ion exchange with micas have been carried out but little or no investigation has been made of heavy-metal ion exchange on the K-depleted micas. The objective of this research was, therefore, to study selective ion-exchange properties of K-depleted micas

(K-depleted phlogopite and biotite) for Co^{2+} and Ni^{2+}. For this purpose, exchange isotherms of Co^{2+} and Ni^{2+} with the K-depleted micas were determined. Kielland plots were also prepared in order to determine the selectivity coefficient. The results obtained in this research could be used as fundamental information to design a water-treatment system for removal of some heavy metals.

MATERIALS AND METHODS

Preparation and characterization of K-depleted biotite and phlogopite

Natural phlogopite and biotite from Bancroft, Ontario, Canada, were procured from Wards Natural Science Establishment, Inc. (Rochester, New York, USA). These micas were wet ground in a blender with deionized water and the <50 μm size fractions were obtained using a standard sieve. K-depleted phlogopite $[Na(Si_3Al)(Mg)_3O_{10}(OH)_2{\cdot}H_2O]$ and K-depleted biotite $[Na(Si_3Al)(Mg,Fe^{2+})_3O_{10}(OH)_2{\cdot}H_2O]$ were produced according to the method of Scott and Smith (1966). The theoretical cation exchange capacities (CEC) of K-depleted phlogopite and biotite are 2.39 and 2.14 meq/g, respectively. A 15 g portion of the <50 μm fraction of natural mica was stirred in a dark bottle containing 300 mL of 1.0 M NaCl-0.2 N sodium tetraphenylborate (NaTPB)-0.01 M disodium ethylenediaminetetraacetic acid (EDTA) solution at room temperature for 1 day. After equilibration, the mica slurry was filtered through Whatman 50 filter paper under vacuum. The solid portion collected was washed with 40% 0.5 N NaCl-60% acetone (volume basis) solution several times. The product was then washed repeatedly with deionized water. This series of procedures was repeated several times to completely remove K from the natural micas. The K-depleted biotite used in this study was provided by the late Dr A.D. Scott. All reagents were of analytical grade and were used without further purification. Powder X-ray diffraction (XRD) analysis was carried out to confirm removal of K from the two natural micas using a Scintag diffractometer with CuKα radiation.

Cation-exchange isotherm determination

Twenty-five mg of the K-depleted phlogopite or biotite (<50 μm size) was placed in a polypropylene centrifuge tube containing 25 mL of a solution with varying fractions (1, 0.75, 0.5, 0.3, 0.2, or 0.1) of $M^{n+}/(Na^+ + M^{n+})$ ($M^{n+} = Co^{2+}$ or Ni^{2+}). The total normality of the equilibrating solutions was kept at 0.00214 for the $2Na^+ \rightarrow Co^{2+}$ and 0.00239 N for $2Na^+ \rightarrow Ni^{2+}$ exchange reactions, respectively. The initial chloride concentration was 0.00214 for the $2Na^+ \rightarrow Co^{2+}$ and 0.00239 N for $2Na^+ \rightarrow Ni^{2+}$ equilibrating solutions, respectively. The batch experiments were carried out in triplicate at room temperature for 4 weeks. In order to avoid precipitation of Co^{2+} or Ni^{2+} during the exchange process, the initial pH of the equilibration solutions was set to 4.5 using HCl solution. The initial and final pH values of the exchange reactions were measured using a pH meter (Orion Research Inc., Beverly, Massachusetts). The separation of solid and solution phases was achieved by centrifugation (HT centrifuge, IEC) at 5000 rpm. Powder XRD analysis of the solid phases was used to monitor changes in the d_{001} spacings. The solutions were analyzed by atomic absorption spectroscopy (AAS) using a Perkin-Elmer Model PE 703 instrument. The measured concentrations of Co^{2+} or Ni^{2+} after exchange reactions were the final concentrations which correspond to data points in the isotherm.

Theoretical

The purpose of this section is to provide a better understanding of cation exchange theory used in this work. The cation exchange between Na^+ and heavy-metal cation ($M^{n+} = Co^{2+}$ or Ni^{2+}) on the K-depleted mica can be represented by,

$$n\bar{\mathrm{Na}}^+ + M^{n+} \rightleftharpoons n\mathrm{Na}^+ + \bar{M}^{n+} \quad (1)$$

According to the Gaines and Thomas thermodynamic treatment (Townsend, 1984), the thermodynamic equilibrium constant, K, is expressed as

$$\mathrm{K} = \frac{\bar{X}_M[\mathrm{Na}^+]^n f_M \gamma^n_{\mathrm{Na}}}{\bar{X}^n_{\mathrm{Na}}[M^{n+}] f^n_{\mathrm{Na}} \gamma_M} \quad (2)$$

where $[Na^+]$ and $[M^{n+}]$ represent the molalities of Na and metal ions in solution, respectively. γ^n_{Na} and γ_M are the activity coefficients of Na and metal ions in the solution, respectively. f^n_{Na} and f_M are the activity coefficients of Na and metal ions in the solid, respectively. $\bar{X}^n_{Na}$ and $\bar{X}_M$ represent the equivalent fractions of Na and metal ion in the solid, respectively. $\bar{X}_i$ is defined by:

$$\bar{X}_{\mathrm{Na}} = \frac{[\overline{\mathrm{Na}}^+]}{n[\bar{M}^{n+}] + [\overline{\mathrm{Na}}^+]}, \quad \bar{X}_M = \frac{n[\bar{M}^{n+}]}{n[\bar{M}^{n+}] + [\overline{\mathrm{Na}}^+]} \quad (3)$$

Equation 2 can be expressed in another way by substituting X_{Na} and X_M for $[Na^+]$ and $[M^{n+}]$, respectively:

$$X_{\mathrm{Na}} = \frac{[\mathrm{Na}^+]}{n[M^{n+}] + [\mathrm{Na}^+]}, \quad X_M = \frac{n[M^{n+}]}{n[M^{n+}] + [\mathrm{Na}^+]} \quad (4)$$

where X_{Na} and X_M represent the equivalent fractions of Na and metal ions in solution, respectively.

Thus, K can be given by:

$$\begin{aligned}\mathrm{K} &= \frac{X^n_{\mathrm{Na}}\bar{X}_M \gamma^n_{\mathrm{Na}} f_M}{X_M \bar{X}^n_{\mathrm{Na}} \gamma_M f^n_{\mathrm{Na}}}[n(\mathrm{TN})^{n-1}] \\ &= \frac{(1-X_M)^n \bar{X}_M \gamma^n_{\mathrm{Na}} f_M}{X_M(1-\bar{X}_M)^n \gamma_M f^n_{\mathrm{Na}}}[n(\mathrm{TN})^{n-1}] \end{aligned} \quad (5)$$

https://doi.org/10.1346/CCMN.2009.0570301 Published online by Cambridge University Press

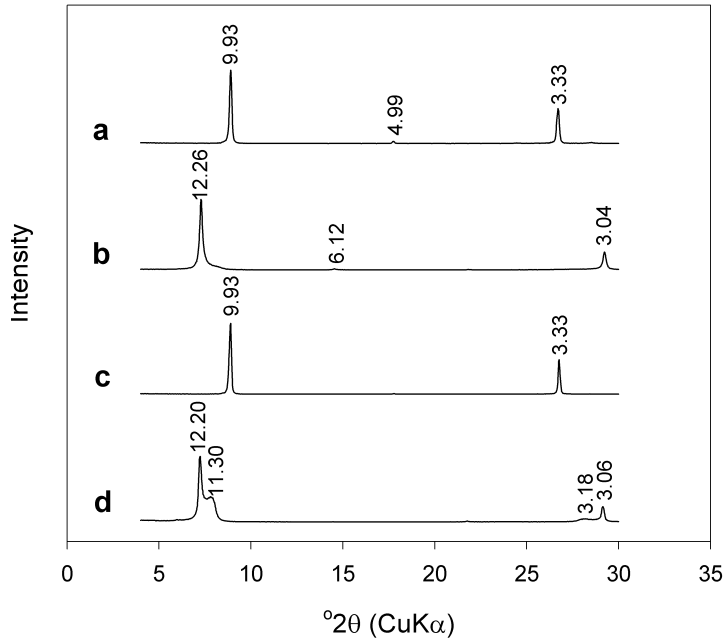

Figure 1. XRD patterns of (a) natural phlogopite, (b) K-depleted phlogopite, (c) natural biotite, and (d) K-depleted biotite. *d* spacing values are given in Å.

In the case of dilute solution, the ratio of γ^n_{Na} to γ_M (γ^n_{Na}/γ_M) is assumed to be 1 (Barrer and Klinowski, 1974), but for mono-divalent exchange reaction, the ionic activity coefficient (γ^n_{Na} or γ_M) cannot be ignored (Singh and Mehrotra, 1989).

In terms of a non-ideal mole fraction effect in a solid, K can be defined by:

$$K = K^M_{Na} \frac{f_M}{f^n_{Na}} \quad (6)$$

where K^M_{Na} is the selectivity coefficient and is defined by:

$$K^M_{Na} = \frac{X^n_{Na}\bar{X}_M\gamma^n_{Na}}{X_M\bar{X}^n_{Na}\gamma_M}[n(TN)^{n-1}] = \frac{(1-X_M)^n\bar{X}_M\gamma^n_{Na}}{X_M(1-\bar{X}_M)^n\gamma_M}[n(TN)^{n-1}] \quad (7)$$

where TN represents total normality in the solution (TN -= $[Na^+] + n[M^{n+}]$).

Table 1. pH values after $2Na^+ \rightarrow Co^{2+}$ or $2Na^+ \rightarrow Ni^{2+}$ exchange reactions.

Solutions for $2Na^+ \rightarrow Co^{2+}$	K-depleted biotite final pH±S.D.[a]	K-depleted phlogopite final pH±S.D.[a]	Solution for $2Na^+ \rightarrow Ni^{2+}$	K-depleted biotite final pH±S.D.[a]	K-depleted phlogopite final pH±S.D.[a]
2.14 mN $CoCl_2$	5.3±0.1	5.4±0.1	2.39 mN $NiCl_2$	5.0±0.0	4.9±0.0
1.605 mN $CoCl_2$ + 0.535 mN NaCl	5.7±0.2	5.8±0.1	1.793 mN $NiCl_2$ + 0.597 mN NaCl	5.4±0.1	5.0±0.1
1.070 mN $CoCl_2$ + 1.070 mN NaCl	6.1±0.1	6.3±0.1	1.195 mN $NiCl_2$ + 1.195 mN NaCl	5.6±0.0	5.7±0.2
0.642 mN $CoCl_2$ + 1.498 mN NaCl	6.4±0.3	6.4±0.3	0.717 mN $NiCl_2$ + 1.673 mN NaCl	6.0±0.1	5.6±0.1
0.428 mN $CoCl_2$ + 1.712 mN NaCl	6.7±0.2	6.4±0.2	0.478 mN $NiCl_2$ + 1.912 mN NaCl	6.2±0.2	5.7±0.3
0.214 mN $CoCl_2$ + 1.926 mN NaCl	6.6±0.3	6.6±0.1	0.239 mN $NiCl_2$ + 2.151 mN NaCl	6.3±0.1	6.1±0.2

Initial pHs of all solutions were set to 4.5
[a]S.D. = standard deviation

https://doi.org/10.1346/CCMN.2009.0570301 Published online by Cambridge University Press

Table 2. Uptake amount of Co^{2+} after cation exchange reaction.

Solution for $2Na^+ \rightarrow Co^{2+}$	Initial Co^{2+} conc. (mN)	— K-depleted phlogopite — Co^{2+} uptake (meq/g)	Co^{2+} at equilibrium conc. (mN)	— K-depleted biotite — Co^{2+} uptake (meq/g)	Co^{2+} at equilibrium conc. (mN)
2.14 mN $CoCl_2$	2.14	1.471	6.67×10^{-1}	1.157	9.81×10^{-1}
1.605 mN $CoCl_2$ + 0.535 mN NaCl	1.605	1.406	1.21×10^{-1}	1.161	3.67×10^{-1}
1.070 mN $CoCl_2$ + 1.070 mN NaCl	1.070	1.052	5.09×10^{-4}	1.022	3.00×10^{-2}
0.642 mN $CoCl_2$ + 1.498 mN NaCl	0.642	0.667	1.24×10^{-3}	0.667	1.92×10^{-3}
0.428 mN $CoCl_2$ + 1.712 mN NaCl	0.428	0.450	9.05×10^{-4}	0.449	2.60×10^{-3}
0.214 mN $CoCl_2$ + 1.926 mN NaCl	0.214	0.212	3.39×10^{-4}	0.212	1.10×10^{-3}

The corrected selectivity coefficient (K^M_{Na}) can be determined by plotting the logarithm of K^M_{Na} (log K^M_{Na}) *vs.* equivalent fraction of metal ion in solid ($\bar{X}_M$). The plot can be expressed as:

$$\log K^M_{Na} = 2C_1\bar{X}_M + \log (K^M_{Na})_{X_M, \bar{X}_M \rightarrow 0} \quad (8)$$

where, C_1 is the Kielland coefficient. If log K^M_{Na} >0, the solid exchanger shows a preference for metal ions, while the exchanger shows a preference for Na ions if <0. No preference exists between these ions if log K^M_{Na} = 0.

RESULTS AND DISCUSSION

Characterization of the K-depleted micas

After the K-removal procedure, the d_{001} spacing value of the natural phlogopite increased from 9.93 to 12.34 Å, resulting in the formation of the K-depleted phlogopite, *i.e.* Na-phlogopite (Figure 1a,b). This increase in the d_{001} spacing resulted from a complete replacement of K^+ with Na^+ and one layer of water molecules in the interlayers. In the case of the biotite (Figure 1c,d), the K-removal treatment resulted in an increase in the d_{001} spacing from 9.93 to 12.20 Å with a shoulder at 11.30 Å. The presence of the shoulder peak at 11.30 Å is due to partial dehydration leading to a smaller number of molecules in the interlayers.

pH change after the $2Na^+ \rightarrow Co^{2+}$ or $2Na^+ \rightarrow Ni^{2+}$ exchange reaction

The pH values of solutions after the $2Na^+ \rightarrow Co^{2+}$ or $2Na^+ \rightarrow Ni^{2+}$ exchange reaction (Table 1) revealed that, in all cases of $2Na^+ \rightarrow Co^{2+}$ exchange reactions with

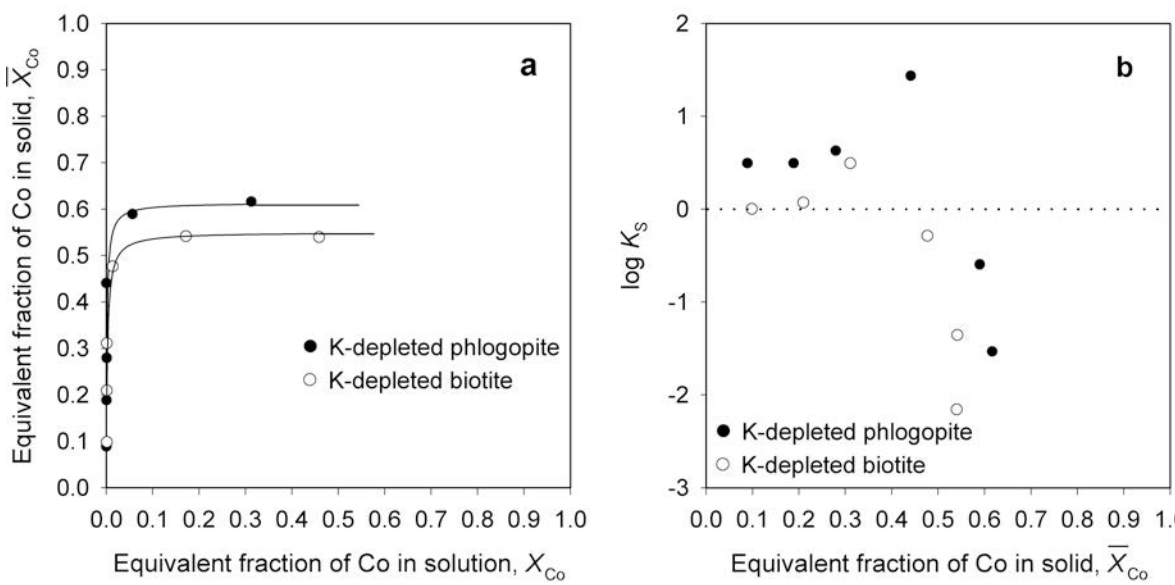

Figure 2. $2Na^+ \rightarrow Co^{2+}$ ion exchange with K-depleted micas: (a) isotherms and (b) Kielland plots ($K_S = K^{Co}_{Na}$).

https://doi.org/10.1346/CCMN.2009.0570301 Published online by Cambridge University Press

different mole fractions of Co^{2+}, the pH values increased after the equilibration. The initial pH for all solutions was set at 4.5. After equilibration, the pH increased to 5.3–6.6 depending on the Co concentration. This increase in pH may be due to the buffering capacity of the K-depleted mica (K-depleted biotite or K-depleted phlogopite). Within the pH range of pH 4.5 to 7.5, cation exchange and protonation or deprotonation on clay minerals function to buffer the pH (McBride, 1994). During the $2Na^+ \rightarrow Co^{2+}$ exchange process, the K-depleted mica consumes H^+ ions in solution by the $Na^+ \rightarrow H^+$ exchange, resulting in the increase in pH. When the K-depleted mica was equilibrated with the large mole fraction of Co^{2+} in solution, the change in pH was less than that where the mole fraction of Co^{2+} in solution was small. In the case of the smallest mole fraction of Co^{2+}, the pH increased to 6.6 for both K-depleted micas. As the mole fraction of Co^{2+}increased, the pH change was smaller. The effect of Co concentration on pH cannot be explained without further study. The *Visual Minteq* program (Gustafsson, 2005) was used to check for precipitation of Co(II), and to predict the distribution of Co(II) species in the equilibration solution. For all equilibration solutions, Co^{2+} was calculated to be the predominant species. *Visual Minteq* also showed no precipitation of Co in any of the equilibration solutions. The pH increased in all equilibration solutions after the $2Na^+ \rightarrow Ni^{2+}$ exchange reactions (Table 1). With increasing Ni^{2+} concentration, the difference between initial and final pH values was less. For all experimental cases, *Visual Minteq* showed that Ni^{2+} was the predominant species and that no precipitation of Ni(II) occurred during the exchange process.

$2Na^+ \rightarrow Co^{2+}$ exchange with K-depleted phlogopite and biotite

The $2Na^+ \rightarrow Co^{2+}$ exchange isotherm with K-depleted phlogopite (Figure 2a), in which each data point was obtained in triplicate and represents the average of a mean variation of <±3%, showed that the K-depleted phlogopite takes up most Co^{2+} from solution at low Co^{2+} concentrations (X_{Co} <0.6). Exchange of Co^{2+} apparently ceased at ~$\bar{X}_{Co}$ >0.6. In addition, the amount of Co^{2+} that replaced Na^+ on the mica after the cation exchange reaction was determined from the isotherm (Table 2).

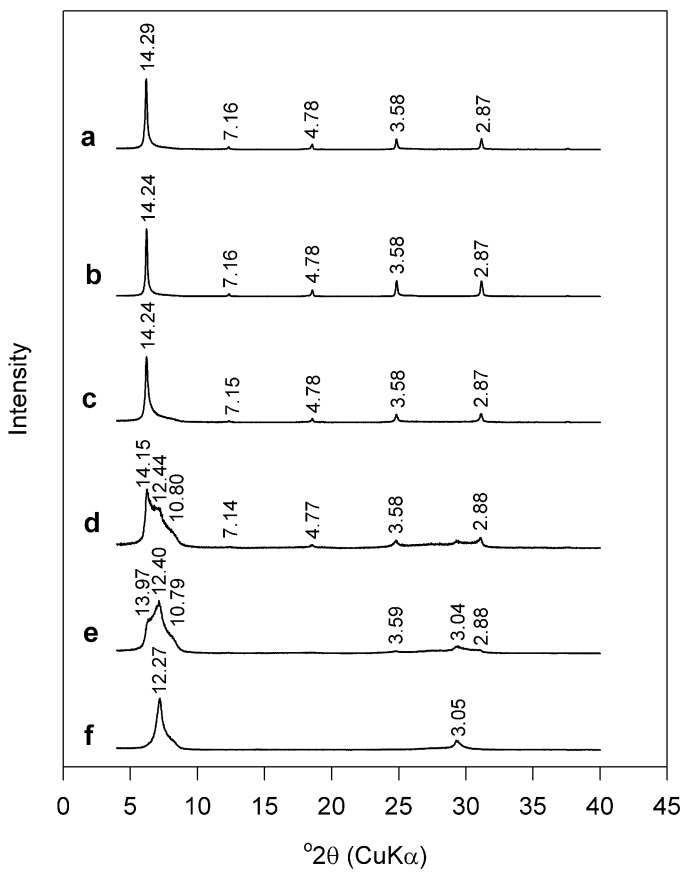

Figure 3. XRD patterns of K-depleted phlogopite after $2Na^+ \rightarrow Co^{2+}$ exchange reaction with (a) 2.14 mN $CoCl_2$, (b) 1.605 mN $CoCl_2$ + 0.535 mN NaCl, (c) 1.070 mN $CoCl_2$ + 1.070 mN NaCl, (d) 0.642 mN $CoCl_2$ + 1.498 mN NaCl, (e) 0.428 mN $CoCl_2$ + 1.712 mN NaCl, and (f) 0.214 mN $CoCl_2$ + 1.926 mN NaCl. *d* spacing values are given in Å.

https://doi.org/10.1346/CCMN.2009.0570301 Published online by Cambridge University Press

A Kielland plot of the data failed to give a good linear relationship because of the scattering of the data (Figure 2b). However, a majority of the data points falls above the dotted line where the selectivity coefficient, K_s, is equal to one. At $\bar{X}_{Co}$ <0.3, the K_s value is small but constant. In the $\bar{X}_{Co}$ range of 0.3 to 0.45, the break point is observed in the Kielland plot. However, in the $\bar{X}_{Co}$ range of 0.45 to 0.62, the K_s value is decreased dramatically.

The XRD patterns after the $2Na^+ \rightarrow Co^{2+}$ exchange reaction with the K-depleted phlogopite using the different Co concentrations (Figure 3) indicate that interlayer collapse was not observed for all exchange reactions. After equilibration with a solution of 0.214 mN $CoCl_2$ and 1.926 mN NaCl, the d_{001} spacing of the original K-depleted phlogopite (12.26 Å) remained the same, *i.e.* 12.27 Å. After equilibration with a solution of 0.428 mN $CoCl_2$ and 1.712 mN NaCl, the d_{001} spacing showed a set of broad peaks at 13.97, 12.40, and 10.79 Å. This broadening of peaks is due to different amounts of Co ions, Na ions, and water molecules in the interlayers. The 13.97 Å peak indicates replacement of Na^+ with Co^{2+} and the presence of extra layers of interlayer water. This ~14 Å peak is due to the difference between the hydrated radii of Co^{2+} (4.23 Å) and Na^+ (3.6 Å) as well as the presence of double sheets of interlayer water (Kodama and Komarneni, 1999). This explanation is reasonable when one assumes that the layer thickness of talc without interlayer cations is ~9.4 Å. A single sheet of interlayer water and Co^{2+} is unlikely to cause the d_{001} spacing of the K-depleted phlogopite to expand to ~14 Å because the ~12 Å peak of the original K-depleted phlogopite is attributed to the presence of Na^+ and a single sheet of interlayer water. After equilibration with a solution of 0.642 mN $CoCl_2$ and 1.498 mN NaCl, the 13.97, 12.40, and 10.79 Å peaks shifted to 14.15, 12.44, and 10.88 Å, respectively. After equilibration with a solution of 1.070 mN $CoCl_2$ and 1.070 mN NaCl, the ~12 and ~11 Å peaks disappeared and the 14.2 Å peak was sharpened (Figure 3c). With regard to the Kielland plot, XRD patterns corresponding to three data points on the Kielland plot at $\bar{X}_{Co}$ <0.3 (Figure 3d,e, and f) show that the K-depleted phlogopite does not have a uniformly single interlayer spacing but irregularly interstratified spacings, except for the lowest Co^{2+} concentration (Figure 3d,e). The spacing of

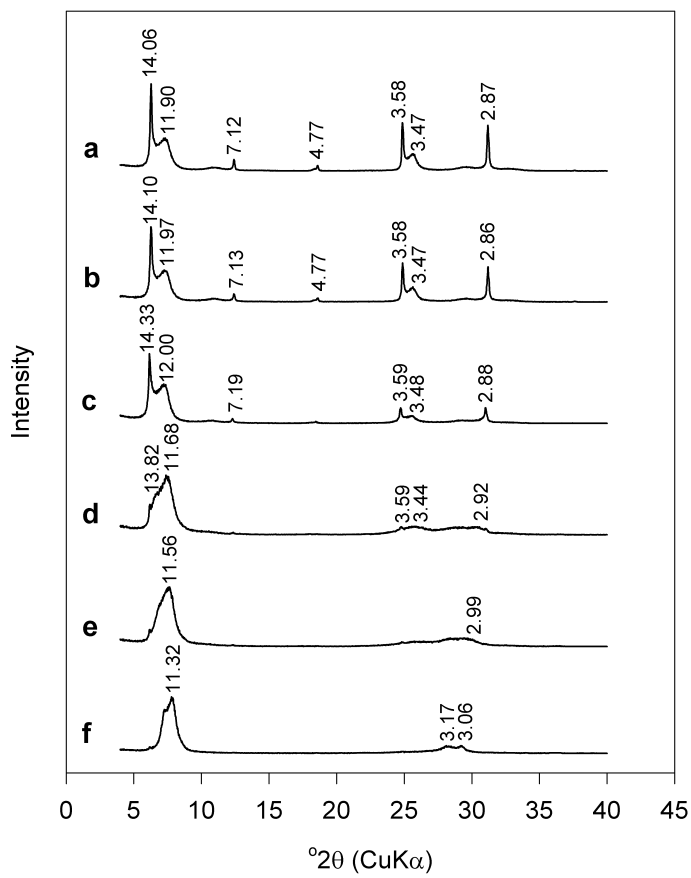

Figure 4. XRD patterns of K-depleted biotite after $2Na^+ \rightarrow Co^{2+}$ exchange reaction with (a) 2.14 mN $CoCl_2$, (b) 1.605 mN $CoCl_2$ + 0.535 mN NaCl, (c) 1.070 mN $CoCl_2$ + 1.070 mN NaCl, (d) 0.642 mN $CoCl_2$ + 1.498 mN NaCl, (e) 0.428 mN $CoCl_2$ + 1.712 mN NaCl, and (f) 0.214 mN $CoCl_2$ + 1.926 mN NaCl. *d* spacing values are given in Å.

https://doi.org/10.1346/CCMN.2009.0570301 Published online by Cambridge University Press

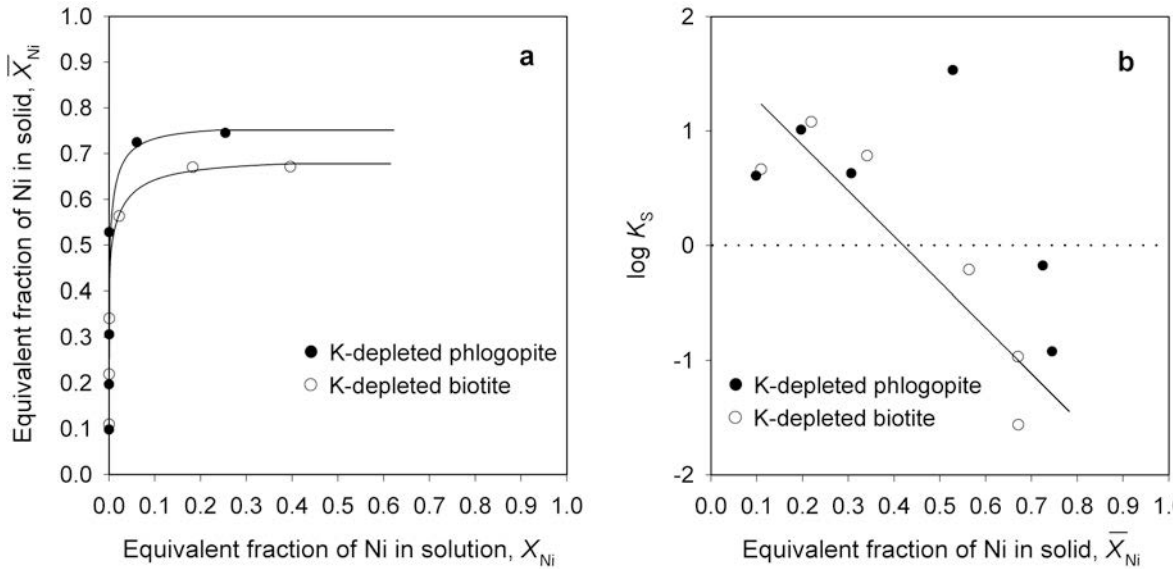

Figure 5. $2Na^+ \rightarrow Ni^{2+}$ ion exchange with K-depleted micas: (a) isotherms and (b) Kielland plots ($K_S = K_{Na}^{Ni}$).

K-depleted phlogopite did not change at the lowest Co^{2+} concentration (Figure 3f) because not enough Co^{2+} ions are present on exchange sites to cause a change in the interlayer spacing. The presence of the irregular multi-interlayer spacings (Figure 3d,e) suggests that the K-depleted phlogopite is probably irregularly interstratified with Na^+ and Co^{2+} ions. In the XRD pattern corresponding to the point at $\bar{X}_{Co}$ = ~0.45 on the Kielland plot (Figure 3c) the d_{001} spacing was 14.24 Å, apparently representing a stable spacing because of enough Co^{2+} ions in the interlayers. These XRD patterns suggest that Co^{2+} ions replace Na^+ ions on the interlayer and planar surfaces, but do not act at the edge sites of the micas. Based on the XRD patterns corresponding to two data points on the Kielland plot in the $\bar{X}_{Co}$ range of 0.5 to 0.62 (Figure 2a,b), K-depleted phlogopite is no longer selective for Co^{2+} even though the hydrated interlayer structure is still retained. This suggests that when a certain amount of Co^{2+} ions occupy the interlayer, a diffusion limitation occurs between Co^{2+} ions which are already present in the interlayer and those that are entering into the interlayer. The diffusion limitation could be deduced from the generalized Kielland coefficients, which are negative when the exchange data within the $\bar{X}_{Co}$ range of 0.5 to 0.62 are fitted to the linear Kielland plot.

The $2Na^+ \rightarrow Co^{2+}$ exchange isotherm with K-depleted biotite (Figure 2a) (each data point based on triplicate runs and being the average of a mean variation of <±4%) revealed that, like the K-depleted phlogopite, the

Table 3. Uptake amount of Ni^{2+} after cation exchange reaction.

Solutions for $2Na^+ \rightarrow Ni^{2+}$	Initial Ni^{2+} conc. (mN)	— K-depleted phlogopite — Ni^{2+} uptake (meq/g)	Ni^{2+} at equilibrium conc. (mN)	— K-depleted biotite — Ni^{2+} uptake (meq/g)	Ni^{2+} at equilibrium conc. (mN)
2.39 mN $NiCl_2$	2.39	1.778	6.08×10^{-1}	1.439	9.46×10^{-1}
1.793 mN $NiCl_2$ + 0.597 mN NaCl	1.793	1.729	1.45×10^{-1}	1.437	4.37×10^{-1}
1.195 mN $NiCl_2$ + 1.195 mN NaCl	1.195	1.260	7.95×10^{-4}	1.208	5.27×10^{-2}
0.717 mN $NiCl_2$ + 1.673 mN NaCl	0.717	0.731	1.70×10^{-3}	0.731	1.48×10^{-3}
0.478 mN $NiCl_2$ + 1.912 mN NaCl	0.478	0.470	3.41×10^{-4}	0.470	3.41×10^{-4}
0.239 mN $NiCl_2$ + 2.151 mN NaCl	0.239	0.235	3.41×10^{-4}	0.235	3.41×10^{-4}

https://doi.org/10.1346/CCMN.2009.0570301 Published online by Cambridge University Press

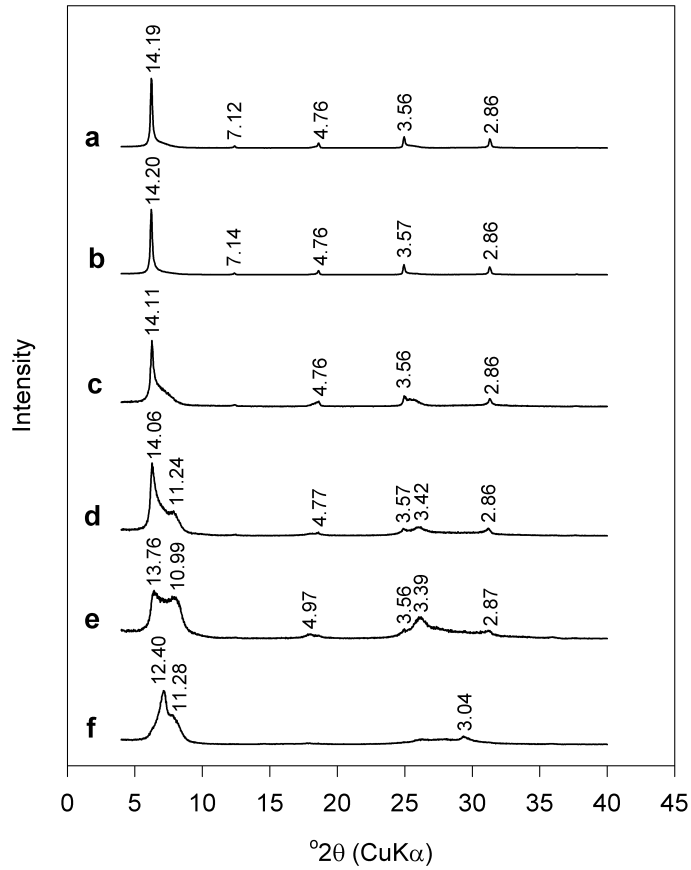

Figure 6. XRD patterns of K-depleted phlogopite after $2Na^{+} \rightarrow Ni^{2+}$ exchange reaction with (a) 2.39 mN $NiCl_2$, (b) 1.793 mN $NiCl_2$ + 0.597 mN NaCl, (c) 1.195 mN $NiCl_2$ + 1.195 mN NaCl, (d) 0.717 mN $NiCl_2$ + 1.673 mN NaCl, (e) 0.478 mN $NiCl_2$ + 1.912 mN NaCl, and (f) 0.239 mN $NiCl_2$ + 2.151 mN NaCl. *d* spacing values are given in Å.

K-depleted biotite takes up most Co^{2+} at $\bar{X}_{Co}$ <~0.48 but takes up no more Co^{2+} at ~$\bar{X}_{Co}$ >0.54. The amount of Co^{2+} that replaced Na^{+} on the K-depleted biotite is determined from the isotherm (Table 2). The Kielland plot for $2Na^{+} \rightarrow Co^{2+}$ exchange with the K-depleted biotite (Figure 2b) did not give a good linear relationship because of the scattering of the data. At $\bar{X}_{Co}$ <0.21, the K_s values are slightly greater than one. In the $\bar{X}_{Co}$ range of 0.3 to 0.54, the K_s values decrease dramatically. Comparing the uptake of Co^{2+} by the K-depleted phlogopite with that of the K-depleted biotite, the amounts of Co^{2+} exchanged on the K-depleted biotite are smaller than those of the K-depleted phlogopite. The difference between the micas in terms of the amounts of Co^{2+} adsorbed may be due to layer-charge density and chemical composition. The total charge density of biotite decreases upon K depletion as a result of Fe oxidation (Sridhar and Jackson, 1974).

The XRD patterns after the $2Na^{+} \rightarrow Co^{2+}$ exchange reaction with the K-depleted biotite using the different Co^{2+} concentrations (Figure 4), unlike the K-depleted phlogopite, show that the collapse of the interlayers occurred at low Co^{2+} concentrations (0.428 mN $CoCl_2$ + 1.712 mN NaCl, and 0.214 mN $CoCl_2$ + 1.926 mN NaCl) (Figure 4e,f). The collapsed 11.32 and 11.56 Å peaks were broadened. This collapse of the interlayer may result in very small K_s values (Figure 2b). After equilibration with a solution of 0.642 mN $CoCl_2$ + 1.498 mN NaCl, a peak appeared at 13.82 Å and the 11.56 Å peak shifted to 11.68 Å. The peak at 13.82 Å may indicate the replacement of Na^{+} by Co^{2+} and the presence of an extra sheet of interlayer water as revealed by XRD patterns (Figure 4d). After equilibration with a solution of 1.070 mN $CoCl_2$ and 1.070 mN NaCl, the 13.82 and 11.68 Å peaks shifted to 14.33 and 12.00 Å, respectively (Figure 4c). The 14.33 Å peak was sharpened and was more intense than that of the 13.82 Å peak. With increasing Co^{2+} concentrations, the ~14 Å peak was sharpened (Figure 4a,b). As for the K-depleted phlogopite, and based on the Kielland plot (Figure 2b), K-depleted biotite is not selective for Co^{2+} at greater Co^{2+} concentrations even though the hydrated interlayer structure (~14 Å) is still retained and can be explained by a severe limitation of further diffusion of Co^{2+} ions.

https://doi.org/10.1346/CCMN.2009.0570301 Published online by Cambridge University Press

$2Na^+ \rightarrow Ni^{2+}$ exchange with K-depleted phlogopite and K-depleted biotite

The $2Na^+ \rightarrow Ni^{2+}$ exchange isotherm with K-depleted phlogopite (Figure 5a) (each data point based on triplicate runs and represents the average of a mean variation of <±3%) shows that the K-depleted phlogopite takes up most Ni^{2+} at low Ni^{2+} concentration but takes up no more Ni^{2+} at $\bar{X}_{Ni} > 0.74$ (74% of the theoretical CEC of the K-depleted phlogopite). The amount of Ni^{2+} that replaced Na^+ on the mica was determined from the isotherm (Table 3). A Kielland plot of the data did not give a good linear relationship because of the scatter of the data points (Figure 5b). However, a majority of the data points falls above the dotted line where the selectivity coefficient, K_s, is equal to one. Although it is difficult to determine a K_s value because of the non-linear relationship, a safe assumption is that the K-depleted phlogopite shows a preference for Ni^{2+} at least up to $\bar{X}_{Ni} < 0.52$.

After the $2Na^+ \rightarrow Ni^{2+}$ exchange reaction with the K-depleted phlogopite using the different Ni^{2+} concentrations, the XRD patterns (Figure 6) showed, as for the $2Na^+ \rightarrow Co^{2+}$ exchange reaction with the K-depleted phlogopite, a splitting of the d_{001} spacing at low Ni^{2+} concentrations.

The $2Na^+ \rightarrow Ni^{2+}$ exchange isotherm with K-depleted biotite (Figure 5a) shows that the K-depleted biotite seems to take up no more Ni^{2+} at $\sim\bar{X}_{Ni} > 0.68$. The amount of Ni^{2+} that replaced Na^+ on the mica is determined from the isotherm (Table 3). Unlike the $2Na^+ \rightarrow Ni^{2+}$ exchange with the K-depleted phlogopite, a Kielland plot for $2Na^+ \rightarrow Ni^{2+}$ exchange with the K-depleted biotite does give a linear relationship (coefficient of determination of linear regression, $r^2 = 0.81$) (Figure 5b). The Kielland coefficient, C_1, was estimated to be −3.979 by plotting log K_S and $\bar{X}_{Ni}$. The negative value of C_1 means that $2Na^+ \rightarrow Ni^{2+}$ exchange becomes more difficult as the exchange progresses (*i.e.* as the number of Ni ions in the interlayer increases). The total amount of Ni^{2+} exchanged on the K-depleted biotite is less than that of the K-depleted phlogopite because of the smaller charge of the former compared to the latter, as explained above.

The $2Na^+ \rightarrow Ni^{2+}$ exchange reaction with the K-depleted biotite, like the $2Na^+ \rightarrow Ni^{2+}$ exchange with

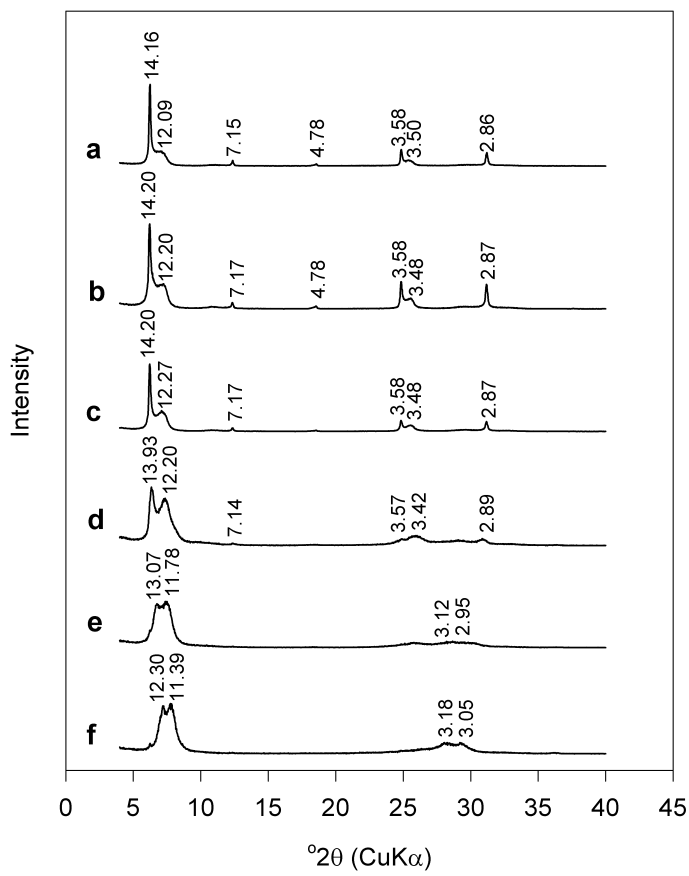

Figure 7. XRD patterns of K-depleted biotite after $2Na^+ \rightarrow Ni^{2+}$ exchange reaction with (a) 2.39 mN $NiCl_2$, (b) 1.793 mN $NiCl_2$ + 0.597 mN NaCl, (c) 1.195 mN $NiCl_2$ + 1.195 mN NaCl, (d) 0.717 mN $NiCl_2$ + 1.673 mN NaCl, (e) 0.478 mN $NiCl_2$ + 1.912 mN NaCl, and (f) 0.239 mN $NiCl_2$ + 2.151 mN NaCl. *d* spacing values are given in Å.

https://doi.org/10.1346/CCMN.2009.0570301 Published online by Cambridge University Press

the K-depleted phlogopite, produced no collapse of the interlayers (Figure 7). With increasing equivalent fraction of Ni^{2+} in solution, the ~14 Å XRD peak was sharpened and its intensity increased (Figure 7a,b,c).

CONCLUSIONS

From the cation exchange isotherm and Kielland plot for $2Na^{+} \rightarrow Co^{2+}$ exchange, the uptake of Co^{2+} by K-depleted phlogopite was ~60% of the theoretical CEC capacity of this phase. For K-depleted biotite, the uptake of Co^{2+} was ~54%. The XRD patterns for $2Na^{+} \rightarrow Co^{2+}$ exchange with K-depleted phlogopite indicated that the hydrated layer spacing of the mica was preserved or expanded to ~14 Å during the exchange process. For the K-depleted biotite, at low $\bar{X}_{Co}$ collapse of the interlayer was observed, but at high $\bar{X}_{Co}$ the d_{001} spacing expanded to ~14 Å. The presence of the ~14 Å spacing indicates that Co^{2+} and double sheets of interlayer water are present in the interlayers.

For the $2Na^{+} \rightarrow Ni^{2+}$ exchange reaction, the uptake of Ni^{2+} by the K-depleted phlogopite was ~74% of the theoretical CEC of the mica. In the case of the K-depleted biotite, the uptake of Ni^{2+} was ~68%. From XRD patterns, the hydrated layer spacings of the micas were preserved or expanded to ~14 Å during the $2Na^{+} \rightarrow Ni^{2+}$ exchange reaction. Both K-depleted micas showed high selectivity for Co^{2+} and Ni^{2+} at lower concentrations of those ions in the presence of greater concentrations of Na^{+} ions.

ACKNOWLEDGMENTS

The authors acknowledge financial support from the Interfacial, Transport, and separation Program, Chemical and Transport Systems Division of the National Science Foundation under Grant No. CTS-0242285, and by the College of Agricultural Sciences, The Pennsylvania State University, under Station Research Project No. PEN03963.

REFERENCES

Aksu, Z. (2002) Determination of the equilibrium, kinetic and thermodynamic parameters of the batch biosorption of nickel(II) ions onto *Chlorella vulgaris*. *Process Biochemstry*, **38**, 89–99.

Barrer, R.M. and Klinowski, J. (1974) Ion-exchange selectivity and electrolyte concentration. *Journal of the Chemical Society, Faraday Transactions 1*, **70**, 2080–2089.

Blanchard, G., Maunaye, M., and Martin, G. (1984) Removal of heavy metals from waters by means of natural zeolites. *Water Research*, **18**, 1501–1507.

Blom, P.E., Johnson, J.B., and Rope, S.K. (1991) Concentrations of 137 Cs and 60 Co in nests of the Harvester ant, Pogonomyrmex salinus, and associated soils near nuclear reactor waste water disposal ponds. *American Midland Naturalist*, **126**, 140–151.

Bortun, A.I., Bortun, L.N., Khainakov, S.A., and Clearfield, A. (1998) Ion exchange properties of the sodium phlogopite and biotite. *Solvent Extraction and Ion Exchange*, **16**, 1067–1090.

Brady, N.C. and Weil, R.R. (2002) *The Nature and Properties of Soils, 13th edition*. Prentice Hall, New Jersey, USA.

Chang, H.-L. and Shih, W.-H. (2000) Synthesis of zeolites A and X from fly ashes and their ion-exchange behavior with cobalt ions. *Industrial & Engineering Chemistry Research*, **39**, 4185–4191.

Charlet, L. and Manceau, A. (1994) Evidence for the neoformation of clays upon sorption of Co(II) and Ni(II) on silicates. *Geochimica et Cosmochimica Acta*, **58**, 2577–2582.

Coleman, N.J., Brassington, D.S., Raza, A., and Mendham, A.P. (2006) Sorption of Co^{2+} and Sr^{2+} by waste-derived 11 Å tobermorite. *Waste Management*, **26**, 260–267.

Crosby, D.G. (1998) *Environmental Toxicology and Chemistry*. Oxford University Press, New York.

Ganesan, V. and Walcarius A. (2004) Surfactant templated sulfonic acid functionalized silica microspheres as new efficient ion exchangers and electrode modifiers. *Langmuir*, **20**, 3632–3640.

Gustafsson, J.P. (2005) *Visual MINTEQ ver. 2.52*. Department of Land and Water Resources Engineering, KTH, Stockholm, Sweden.

Killey, R.W.D., McHugh, J.O., Champ, D.R., Cooper, E.L., and Young, J.L. (1984) Subsurface Cobalt-60 Migration from a Low-Level Waste Disposal Site. *Environmental Science and Technology*, **18**,146–157.

Kodama, T. and Komarneni, S. (1999) Na-4-mica: Cd^{2+}, Ni^{2+}, Co^{2+}, Mn^{2+} and Zn^{2+} ion exchange. *Journal of Materials Chemistry*, **9**, 533–539.

Komarneni, S. and Roy, R. (1988) A cesium selective ion sieve made by topotactic leaching. *Science*, **23**, 1286–1288.

Lv, L., Tsoi, G., and Zhao, X. S. (2004) Uptake equilibria and mechanisms of heavy metal ions on microporous titanosilicate ETS-10. *Industrial & Engineering Chemistry Research*, **43**, 7900–7906.

McBride, M.B. (1994) *Environmental Chemistry of Soils*. Oxford University Press, New York.

Means, J.L., Crerar, D.A., Borcsik, M.P., and Duguid, J.O. (1978a) Adsorption of Co and selected Actinides by Mn and Fe oxides in soils and sediments. *Geochimica et Cosmochimica Acta*, **42**, 1763–1773.

Means, J.L., Crerar, D.A., and Duguid, J.O. (1978b) Migration of radioactive wastes: radionuclide mobilization by complexing agents. *Science*, **200**, 1477–1481.

Netzer, A. and Hughes, D. E. (1984) Adsorption of copper, lead and cobalt by activated carbon. *Water Research*, **18**, 927–933.

Olsen, C.R., Lowry, P.D., Lee, S.Y., Larsen, I.L., and Cutshall, N.H. (1986) Geochemical and environmental processes affecting radionuclide migration from a formerly used seepage trench. *Geochimica et Cosmochimica Acta*, **50**, 593–607.

Rengaraj, S. and Moon, S.-H. (2002) Kinetics of adsorption of Co(II) removal from water and wastewater by ion exchange resins. *Water Research*, **36**, 1783–1793.

Schlegel, M.L., Charlet, L., and Manceau, A. (1999) Sorption of metal ions on clay minerals. II. Mechanism of Co sorption on hectorite at high and low ionic strength and impact on the sorbent stability. *Journal of Colloid and Interface Science*, **220**, 392–405.

Scott, A.D. and Smith, S.J. (1966) Susceptibility of interlayer potassium in micas to exchange with sodium. *Clays and Clay Minerals*, **20**, 93–100.

Singh, D.K. and Mehrotra, P. (1989) Ion-exchange equilibria of metal ions and hydrogen ions on anilinium tin(IV) phosphate. *Transition Metal Chemistry*,, **14**, 119–122.

Sridhar, K. and Jackson, M.L. (1974) Layer charge decrease by tetrahedral cation removal and silicon incorporation during natural weathering of phlogopite and saponite. *Soil Science Society of America Proceedings*, **38**, 847–850.

Stout, S.A., Cho, Y., and Komarneni, S. (2006) Uptake of

cesium and strontium cations by potassium-depleted phlogopite. *Applied Clay Science*, **31**, 306–313.

Strelko, V. and Malik, D.J. (2002) Characterization and metal sorptive properties of oxidized active carbon. *Journal of Colloid and Interface Science*, **250**, 213–220.

Suraj, G., Iyer, C.S.P., and Lalithambika, M. (1998) Adsorption of cadmium and copper by modified kaolinites. *Applied Clay Science*, **13**, 293–306.

Townsend, R.P. (1984) Thermodynamics of ion exchange in clays. *Philosophical Transactions of the Royal Society, A*, **311**, 301–314.

(*Received 29 May 2008; revised 19 January 2009; Ms. 0167; A.E. F. Bergaya*)